

# Investigation of the thermomechanical properties of a plasma-sprayed nanostructured zirconia coating

Huang Chen\*, Xiaming Zhou, Chuanxian Ding

*Shanghai Institute of Ceramics, Chinese Academy of Sciences, Shanghai, 200050, PR China*

Received 16 June 2002; received in revised form 18 September 2002; accepted 28 September 2002

## Abstract

Yttria partially stabilized nanostructured zirconia coatings were deposited by atmospherical plasma spraying (APS). The microstructure of the as-sprayed nanostructured coating was characterized with Scanning electronic microscopy (SEM), Transmission electron microscopy (TEM), X-ray diffraction (XRD) and Raman spectrum (RS). The laser-flash diffusivity method and push-rod method were used to examine the thermomechanical properties of the nanostructured zirconia coatings. The results obtained indicated that the plasma-sprayed zirconia coating possessed nano-structure and its average grain size was about 73 nm. The average thermal expansion coefficients of the nanostructured coating at the first thermal cycle and second thermal cycle from room temperature to 1200 °C are 11.0 and  $11.6 \times 10^{-6} \text{ °C}^{-1}$ , respectively. The thermal diffusivity of the nanostructured zirconia coating was  $1.80\text{--}2.54 \times 10^{-3} \text{ cm}^2/\text{s}$  between 200 and 1200 °C. The microhardness of the nanostructured zirconia coating was 8.6 GPa, which was 1.6 times as large as that of traditional zirconia coating.

© 2002 Elsevier Science Ltd. All rights reserved.

*Keywords:* Hardness; Microhardness; Plasma spraying; Thermal barrier coatings; Thermal diffusivity; Thermal expansion; ZrO<sub>2</sub>

## 1. Introduction

Plasma-sprayed thermal barrier coatings (TBCs) were traditionally applied to gas turbine engines blades and vanes in order to reduce their operating temperatures and increase the component durability. Zirconia-based coatings were commonly used as TBCs because of their low thermal conductivity and high coefficient of thermal expansion.<sup>1–4</sup> Recently, the preparation of nanostructured zirconia coating has become an active field in thermal spray industry.<sup>5–9</sup> It was reported that the development of yttria stabilized nanostructured zirconia coatings might enhance the performance of TBCs due to low thermal conductivity, high coefficient of thermal expansion and excellent mechanical properties of this kind coating.<sup>8,9</sup>

In this paper, an interest has been taken in the thermophysical properties of plasma-sprayed nanostructured zirconia coating, because it is possible to be used at extremely high temperatures and severe thermal

loads in future. The service life of plasma-sprayed TBC is closely related to thermal shock resistance and the thermal expansion mismatch strains, etc.<sup>2–4</sup> There are many reports on the determination of thermophysical properties of plasma-sprayed traditional zirconia coatings, deposited with sintered and crushed micrometer zirconia powder.<sup>3,10–15</sup> However, few reports on plasma-sprayed nanostructured zirconia coatings have been published.

The purpose of the present paper was to investigate the thermophysical properties and the Vickers microhardness of the plasma-sprayed nanostructured zirconia coating. Since the thermomechanical properties of the coating are tightly related to its microstructure, the phase composition and the grain size of the as-sprayed coating were identified also.

## 2. Experimental procedures

### 2.1. preparation of nanostructured zirconia coating

A 3 mol% Y<sub>2</sub>O<sub>3</sub> partially stabilized nanostructured zirconia powder, having grain size of 50–120 nm, was

\* Corresponding author. Tel.: +86-21-5241-4111; fax: +86-21-5241-3903.

E-mail address: [jx\\_chuang@yahoo.com](mailto:jx_chuang@yahoo.com) (H. Chen).

used as the starting powder and was reconstituted into spherical micrometer-sized granules (typical size range in 15–45  $\mu\text{m}$ ) by spray-drying process before plasma spraying in this experiment. A Metco A-2000 atmospheric plasma spraying equipment (Sulzer Metco AG, Switzerland) was selected to spray the nanostructured zirconia coating. During the spraying process, the substrates were cooled by circulating water and surfaces of the coatings were cooled by compressed air. The final coatings with thickness of 1.5–3.0 mm were sprayed onto an aluminum plate of 9 mm  $\times$  14 mm  $\times$  3 mm. Several samples were cut from these coatings for the following measurements of thermophysical properties. Table 1 summarizes the parameters for plasma spraying.

## 2.2. Microstructure analysis

The phase structure of the starting powders and the as-sprayed coating were identified with an RAX-10 X-ray diffractometer (Rigaku, Tokyo, Japan) and a LabRam-1B Micro-Raman spectrometer (Dilor, France). The microstructures of the nanostructured zirconia coatings were determined with an EPMA-8705QH<sub>2</sub> electron probe analyzer (Shimadzu, Tokyo, Japan) and a JEM-200CX transmission electron microscopy (Jeol, Tokyo, Japan). The dependence of grain size of nanostructured zirconia coating on the heat-treating

Table 1  
Plasma-spray parameters for nanostructured zirconia coating

|                                 |     |
|---------------------------------|-----|
| Primary Ar (slpm)               | 42  |
| Secondary H <sub>2</sub> (slpm) | 12  |
| Carrier Ar (slpm)               | 3.5 |
| Gun current (amp)               | 620 |
| Gun voltage (V)                 | 73  |
| Spray distance (mm)             | 120 |

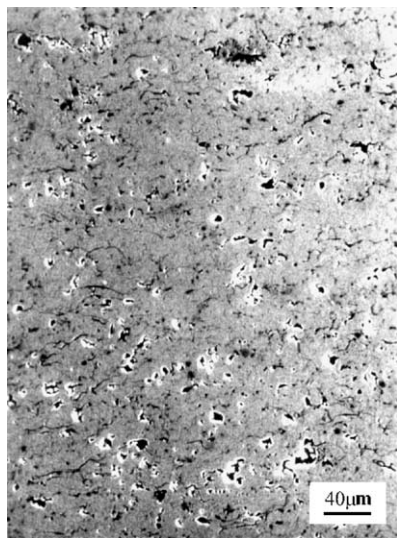


Fig. 1. The typical SEM microstructure of the as-sprayed nanostructured zirconia coating.

temperature was also explored using X-ray diffraction (XRD).

## 2.3. Coefficient of thermal expansion

Thermal expansion measurements of the as-sprayed nanostructured zirconia coating were carried out in air using a high-temperature electronic dilatometer (Model 402ES-3, Netzsch, Germany). The coating samples were 5 mm  $\times$  50 mm  $\times$  2 mm. Heating rates of 5  $^{\circ}\text{C}/\text{min}$  and heating temperature range 25–1200  $^{\circ}\text{C}$  were used. Values of fractional length changes,  $\Delta l/l$ , were obtained and the coefficients of thermal expansion,  $\alpha$ , were calculated. The second measurement was carried out using the same sample after cooled to room temperature.

## 2.4. Thermal diffusivity

The samples were machined to disk shape (10.2 mm in diameter and 1.3 mm in thickness) along the direction parallel to the coating surface for thermal diffusivity measurements. The laser-flash diffusivity method was used to explore the thermal diffusivity in the temperature from 200 to 1200  $^{\circ}\text{C}$ . In order to assure complete absorption of the laser-flash at the sample surface and measurement of the transient temperature at the opposite surface, the coating samples were coated with a carbon film before the measurement. During the process of cooling to room temperature, the thermal diffusivity of the same coating sample was also measured. For comparison, the traditional zirconia coating sprayed at the same parameters as nanostructured zirconia coating was also measured.

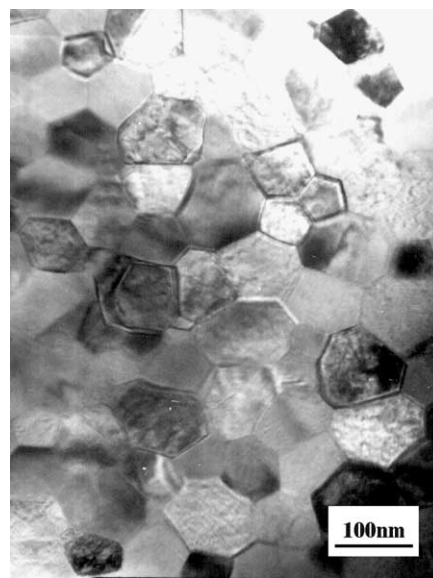
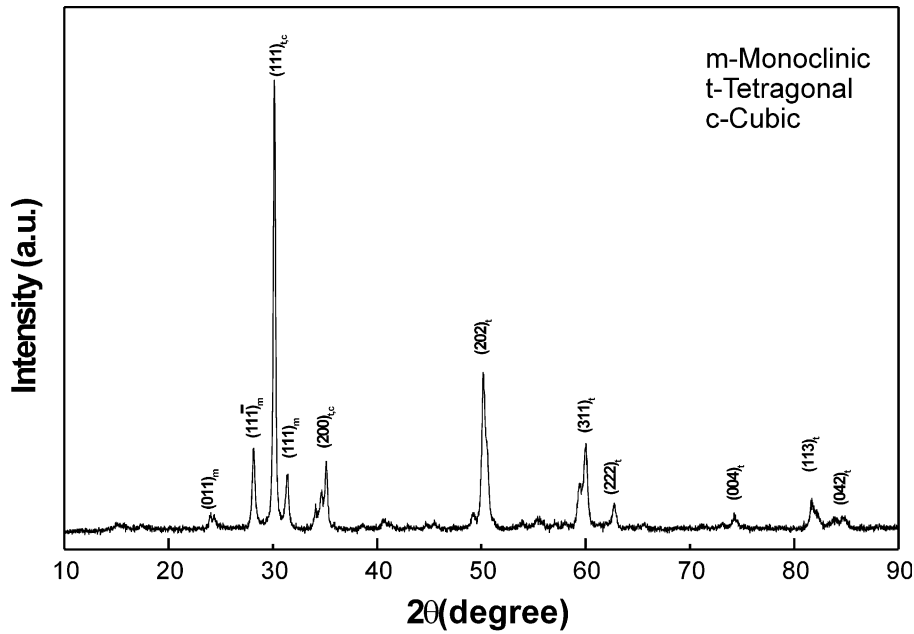
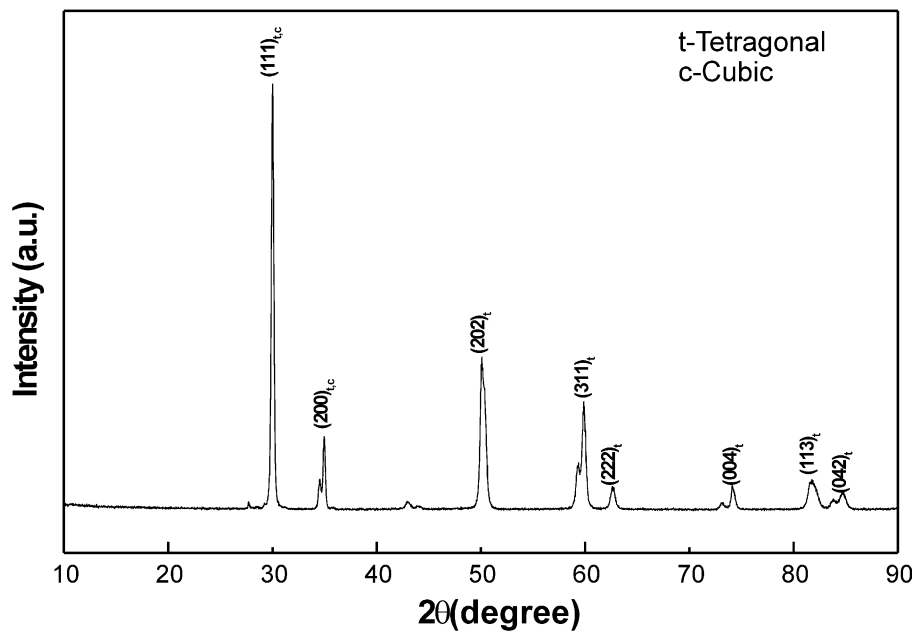


Fig. 2. Transmission electron micrograph of the nanostructured zirconia coating.



(a) starting powder



(b) zirconia coating

Fig. 3. XRD spectra of the starting powders and the as-sprayed coating.

### 2.5. Microhardness evaluation

The Vickers microhardness of the as-sprayed zirconia coatings were measured at 25 randomly located positions on the polished cross section for every sample by a HX-1000 Microhardness Tester. The Vickers microhardness value came from the average of 25 points. To void

the effect of stress field, the distance between two indentations was kept greater than 3 times the indentation diagonal.<sup>16</sup> The measured condition of Vickers microhardness as follow: under load of 1.96 N and loading time of 15 s. The traditional zirconia coatings plasma sprayed at the same parameters as nanostructured zirconia coatings were measured also for comparison.

### 3. Results and discussion

#### 3.1. Microstructure analysis

Fig. 1 presents the typical SEM microstructures of the as-sprayed nanostructured zirconia coatings. It can be seen that the pores are isolated and homogeneous distribution in the coatings. Most of them are less than 10  $\mu\text{m}$ . Transmission electron microscopy image reveals that the coatings are composed of fine grains with size ranging from 30 to 110 nm, as shown in Fig. 2. Phase identification of the nanostructured zirconia coating was carried out using X-ray Diffraction (XRD) with  $\text{CuK}\alpha$  radiation and Raman spectroscopy.

Fig. 3 shows XRD spectra of starting powder and as-sprayed coating. It can be seen that monoclinic phase zirconia, contained in the starting powders (see Fig. 3a), was transferred to tetragonal phase zirconia after the plasma spraying. There isn't a monoclinic phase in the

as-sprayed zirconia coating as shown in Fig. 3b. The Raman spectrum of the as-sprayed coating, as shown in Fig. 4, confirmed this conclusion. Fig. 4 also indicated that the as-sprayed nanostructured zirconia coating was consisted of tetragonal phase zirconia because its spectra were dominated by the relatively sharp tetragonal Raman modes.<sup>17,18</sup>

The volume-average grain size of the as-sprayed coating and the coatings treated at 900, 1000, 1100, and 1200  $^{\circ}\text{C}$  for 2 h were determined from XRD peak broadening [e.g. the  $(111)_t$ ] using the Scherrer equation:<sup>19,20</sup>

$$B_p(2\theta) = 0.9\lambda/D\cos\theta$$

where  $D$  is the average dimensions of crystallite,  $B_p(2\theta)$  is the broadening of the diffraction line measured half maximum intensity,  $\lambda$  is the wavelength of the X-ray

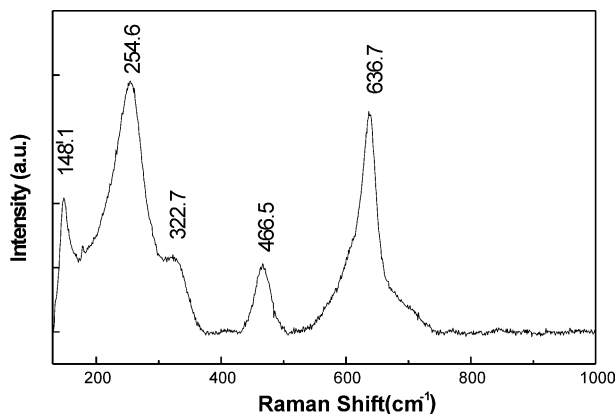


Fig. 4. Raman spectrum of the nanostructured zirconia coating.

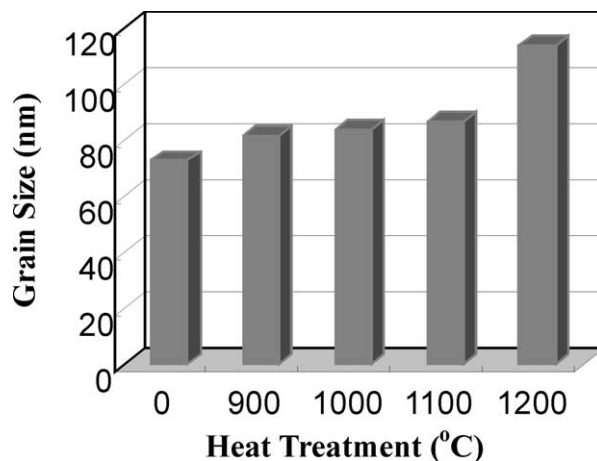


Fig. 5. The average grain size of zirconia for heat treating for 2 h at different temperatures.

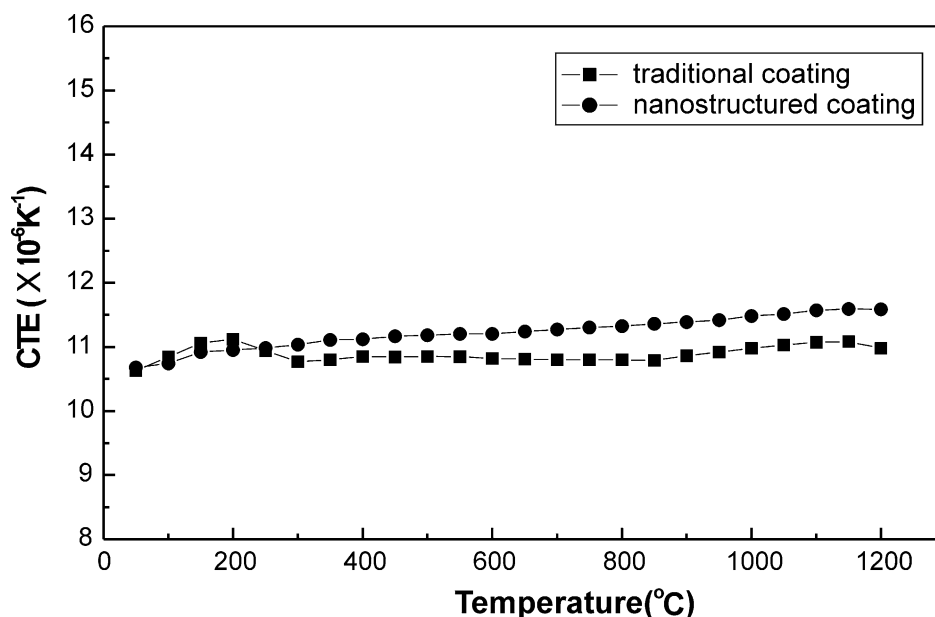


Fig. 6. Coefficient of thermal expansion of the nanostructured zirconia coating.

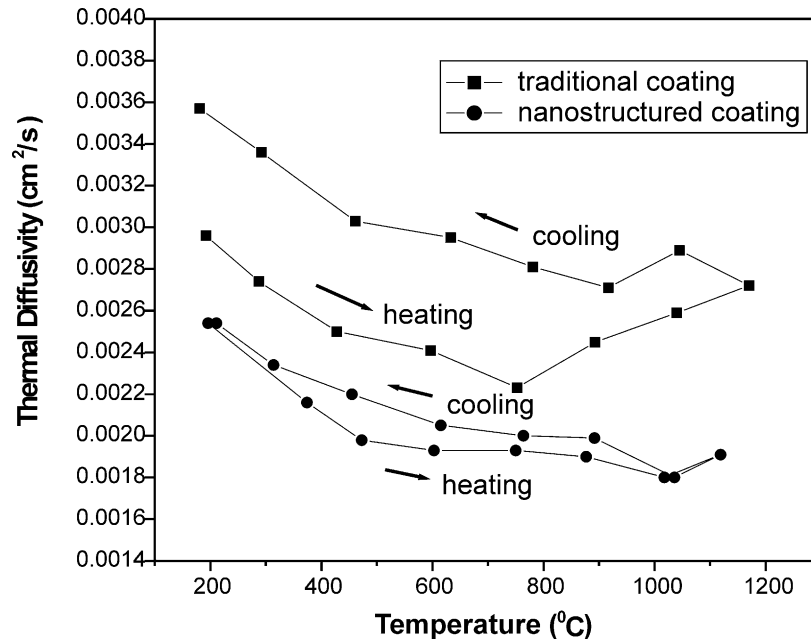


Fig. 7. Thermal diffusivity of the as-sprayed nanostructured and traditional zirconia coatings.

radiation and  $\theta$  is the Bragg angle. The correction for instrumental broadening was taken into account in the measurement of the peak broadening. In this study, this was done by comparing the width at half-maximum intensity of the X-ray reflections between the sample and the single-crystalline Si standard whose diameter is larger than  $10^{-4}$  cm.

$$B_p^2(2\theta) = B_h^2(2\theta) - B_f^2(2\theta) \quad \text{or} \quad B_p(2\theta) = B_h(2\theta) - B_f(2\theta)$$

In the above equation,  $B_p(2\theta)$  is the half-maximum width if there was no instrumental broadening, and  $B_h(2\theta)$  and  $B_f(2\theta)$  are the width of the coating samples and the crystalline Silicon standard, respectively.

Fig. 5 presents the average grain size calculated using Scherrer equation of the as-sprayed coating and the coatings treated at 900, 1000, 1100, and 1200 °C. Fig. 5 indicates that the grain size of nanostructured zirconia coatings increases slowly at temperature less than 1100 °C, then increase quickly with increasing temperature. The average grain size is about 73 nm, which coincided with the observation of transmission electron microscopy. The formation of nano-structure in the plasma sprayed zirconia coating was resulted from the high heating rate of plasma spraying process, short residence time in the plasma jet and high cooling rate of the powder particles.<sup>6,7</sup> There isn't enough time to grow up for nano-scale grains.

### 3.2. Coefficients of thermal expansion (CTE)

Fig. 6 shows thermal expansion coefficient of nanostructured zirconia coating. The average thermal

expansion coefficient of the zirconia coatings at the first thermal cycle and second thermal cycle from room temperature to 1200 °C are 11.0 and  $11.6 \times 10^{-6}$  °C<sup>-1</sup>, respectively. The thermal expansion coefficient of the zirconia coating increased firstly and then decreased from room temperature to 300 °C in the first thermal cycle. This behavior is ascribed to the oxygen loss phenomenon in ceramic coatings prepared by atmospheric plasma spraying.<sup>21,22</sup> When the as-sprayed zirconia coating was heated in atmosphere, the oxygen atoms were added to the vacancies of the coating again. The phenomenon was disappeared in second thermal cycle. During the second thermal cycle, the coefficient of thermal expansion increased linearly with increasing temperature.

### 3.3. Thermal diffusivity

Fig. 7 presents the thermal diffusivity of nanostructured and traditional zirconia coatings during the temperature from 200 to 1200 °C. It can be seen that the thermal diffusivities of both nanostructured and traditional zirconia coatings decreases slightly with an increase in temperature. The thermal diffusivity of the nanostructured zirconia coating was  $1.80\text{--}2.54 \times 10^{-3}$  cm<sup>2</sup>/s in the measured temperature range, while the thermal diffusivity of traditional zirconia coating was  $2.25\text{--}3.57 \times 10^{-3}$  cm<sup>2</sup>/s. And compared with the published thermal diffusivity data of traditional plasma sprayed zirconia coating,<sup>12–14</sup> it can be concluded that the plasma-sprayed nanostructured zirconia coating exhibited lower thermal diffusivity. It was explained in terms of the reduced grain size and the optimized pore

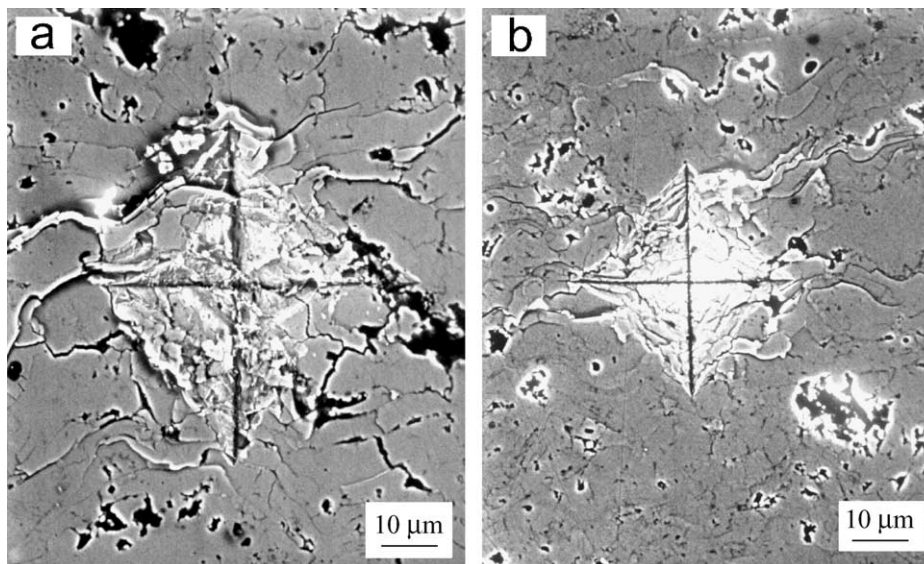


Fig. 8. SEM micrographs showing indent in zirconia coatings.

size of nanostructured zirconia coatings.<sup>8,23,24</sup> The smaller the grain size, the larger the boundary volume and the easier the phonon scattering at grain and layer boundaries.<sup>8</sup> The reduced thermal diffusivity was also benefited from the homogeneous distribution of pores in the plasma sprayed nanostructured zirconia coating.

### 3.4. Microhardness evaluation

The average Vickers microhardness measured at cross-section area of the as-sprayed nanostructured zirconia coating was up to 8.6 GPa, which was about 1.6 times as large as that of traditional zirconia coating deposited at the same conditions. Fig. 8 shows the SEM micrographs of the indents of traditional and nanostructured zirconia coatings. Comparing Fig. 8a with b, it was found that less cracks and thinner indenter major diagonal were appeared on the surface of nanostructured zirconia coating after the identification, which indicated that the toughness of nanostructured zirconia coating was enhanced correspondingly with the great increasing of microhardness.<sup>25</sup>

## 4. Conclusions

The nanostructured zirconia coatings were deposited by atmospherical plasma spraying. The results of X-ray diffraction and Raman spectrum revealed that the plasma-sprayed nanostructured zirconia coating was composed of tetragonal zirconia phase. The as-sprayed coatings were composed of fine grain size ranging from 30 to 110 nm. The average size of the as-sprayed coating was about 73 nm. The Vicker microhardness of the as-sprayed nanostructured zirconia coating was 8.6 GPa, which was about 1.6 times as large as that of traditional

zirconia coating. Thermophysical properties of the as-sprayed nanostructured zirconia coating, such as thermal expansion, thermal diffusivity were measured. The obtained results revealed that the coating exhibited low thermal diffusivity ( $1.80\text{--}2.54 \times 10^{-3} \text{ cm}^2/\text{s}$ ) and high thermal expansion coefficient ( $11.0\text{--}11.6 \times 10^{-6} \text{ }^\circ\text{C}^{-1}$ ).

## Acknowledgements

The authors would like to thank Prof. Tonggen Xi and Dr. Huaqin Xie of SICCAS for the thermophysical properties testing and significant discussion in thermophysical properties.

## References

1. Miller, R. A., Current status of thermal barrier coatings—an overview. *Surf. Coat. Technol.*, 1987, **30**, 1–11.
2. Tamura, M., Takahashi, M., Ishii, J., Suzuki, K., Sato, M. and Shimomura, K., Multilayered thermal barrier coating for land-based gas turbines. *J. Thermal Spray Technol.*, 1999, **8**(1), 68–72.
3. Khor, K. A. and Gu, Y. W., Thermal properties of plasma-sprayed functionally graded thermal barrier coatings. *Thin Solid Films*, 2000, **372**, 104–113.
4. Miller, R. A., Oxidation-based model for thermal barrier coating life. *J. Am. Ceram. Soc.*, 1984, **67**(8), 517–521.
5. Lima, R. S., Kucuk, A. and Berndt, C. C., Evaluation of microhardness and elastic modulus of thermally sprayed nanostructured zirconia coatings. *Surf. Coat. Technol.*, 2001, **135**, 166–172.
6. Zeng, Y., Lee, S. W., Gao, L. and Ding, C. X., Atmospheric plasma sprayed coatings of nanostructured zirconia. *J. Eur. Ceram. Soc.*, 2002, **22**, 347–351.
7. Chen H., Zeng Y. and Ding C. X., Microstructural characterization of plasma-sprayed nanostructured zirconia powders and coatings. *J. Eur. Ceram. Soc.* (in press).
8. Gell, M., Application opportunities for nanostructured materials and coatings. *Mater. Sci. Eng.*, 1995, **A204**, 246–251.

9. Kear, B. H. and Skaudan, G., Thermal spray processing of nanoscale materials. *Nanostruct. Mater.*, 1997, **8**, 765–769.
10. Rangaswamy, S. and Herman, H., Thermal expansion study of plasma-sprayed oxide coatings. *Thin Solid Films*, 1980, **73**, 43–52.
11. Lee Y.-K., Kim H.-J. and Chang R.-W., Thermal expansion properties of plasma-sprayed thick coatings. In *Proceeding of the 15th International Thermal Spray Conference*, 25–29 May, 1998, Nice, France, pp. 1629–1634.
12. Taylor, T. A., Thermal properties and microstructure of two thermal barrier coatings. *Surf. Coat. Technol.*, 1992, **54-55**, 53–57.
13. Taylor, R. E., Wang, X. and Xu, X., Thermomechanical properties of thermal barrier coatings. *Surf. Coat. Technol.*, 1999, **120-121**, 89–95.
14. Pawlowski, L., Lombard, D. and Fauchais, P., Structure-thermal properties-relationship in plasma sprayed zirconia coatings. *J. Vac. Sci. Technol.*, 1985, **A3**, 2494–2500.
15. Gu, S., Lu, T. J., Hass, D. D. and Wadley, N. G., Thermal conductivity of zirconia coatings with zig-zag pore microstructures. *Acta Mater.*, 2001, **49**(13), 2539–2547.
16. Leigh, S., Lin, A. and Berndt, C. C., Elastic response of thermal spray deposits under indentation tests. *J. Am. Ceram. Soc.*, 1997, **80**(8), 2093–2099.
17. Alzyab, B., Perry, C. H. and Ingel, R. P., High-pressure phase transitions in zirconia and yttria-doped zirconia. *J. Am. Ceram. Soc.*, 1987, **70**(10), 760–765.
18. Perry, C. H., Liu, D.-W. and Ingel, R. P., Phase characterization of partially stabilized zirconia by Raman spectroscopy. *J. Am. Ceram. Soc.*, 1985, **68**(8), C184–C187.
19. Klug, H. P. and Alexander, L. E., *X-ray Diffraction Procedures for Polycrystalline and Amorphous Materials*. John Wiley & Sons, Inc, London, 1954.
20. Shaw, L. L., Goberman, D., Ren, R., Goberman, D., Ren, R. M., Gell, M., Jiang, S., Wang, Y., Xiao, T. D. and Strutt, P. R., The dependency of microstructure and properties of nanostructured coatings on plasma spray conditions. *Surf. Coat. Technol.*, 2000, **130**, 1–8.
21. Ramachandran, K., Selvarajan, V., Ananthapadmanabhan, P. V. and Sreekumar, K. P., Microstructure, adhesion, microhardness, abrasive wear resistance and electrical resistivity of the plasma sprayed alumina and alumina-titania coatings. *Thin Solid Films*, 1998, **315**, 144–152.
22. Safai, S. and Herman, H., *Plasma Sprayed Materials: Treaties on Material Science and Technology*. Academic Press, New York, 1981.
23. Hasselman, D. P. H., Johnson, L. F., Bentsen, L. D., Syed, R., Lee, H. L. and Swain, M., Thermal diffusivity and conductivity of dense polycrystalline ZrO<sub>2</sub> ceramics: a survey. *Am. Ceram. Soc. Bull.*, 1987, **66**(5), 799–806.
24. Berndt, C. and Larernia, E. J., Thermal spray processing of nanoscale materials. *J. Thermal Spray Technol.*, 1998, **7**(3), 411–440.
25. Beshish, G. K., Florey, C. K., Worzala, F. J. and Lenling, W. J., Fracture toughness of thermal spray ceramic coatings determined by the indentation technique. *J. Thermal Spray Technol.*, 1993, **2**(1), 35–38.